Chapter 3

Collider Technical Systems

3.1 Overview

This chapter presents details of those technical infrastructure systems for which substantial research and development is required. It is known that it will be possible to scale up many systems from LHC for use in FCC-hh and these systems are not presented below. Various major systems such as magnets, cryogenics, RF, beam transfer and vacuum are described here as well as many smaller essential devices. Finally there is a description of the radiation environment in which they will have to perform. Details for all technical systems will be presented at a later stage in the design process but systems which require particular attention at this conceptual design stage have been identified and are presented here.

3.2 Main Magnet System

3.2.1 Introduction

The magnetic system of the FCC-hh will profit strongly from the experience gained with the LHC, which has demonstrated the feasibility and effectiveness of operating a large number of superconducting magnets cooled by using superfluid helium at 1.9 K. There will be about four times more magnets in FCC-hh than in LHC and the field amplitude produced by the arc dipoles will be increased by almost a factor of two, whilst maintaining a similar beam aperture and twin configuration. The field increase will be enabled by using Nb_3Sn superconductor instead of the Nb-Ti used in the LHC arc dipoles. With respect to the conductor properties, the FCC-hh magnets will operate in a similar condition than the LHC magnets, with 14% margin on the load line and at about 60% of the maximum upper critical field B_{c20}. It is believed that, with an appropriate R&D program, and if all magnets are cold tested before installation, this margin will be sufficient to achieve the nominal energy of the FCC-hh with limited magnet training. This technology, though not yet used in particle colliders, is being implemented for dipoles and quadrupoles of the HL-LHC project, where they will be operating at peak fields of between 11 and 12 T. One can expect that this technology will be ready to start mass production of 16 T magnets within a decade from the manufacture of a first long model.

3.2.2 Superconducting Main Dipole

The main dipoles (MD) of the FCC are twin-aperture magnets of cosine-theta coil layout assembled in a helium-tight cold mass (CM) structure, integrated in a cryostat. A cross section of the system is presented in Fig. 3.1 and a 3D of the assembly is shown in Fig. 3.2.

The CM for the FCC MD is straight, and has a total length between the two extremities of the beam pipe flanges of 15.8 m and a magnetic length of 14.069 m. Its external diameter is 800 mm. It is installed in a cryostat structure composed of a radiation shield, a thermal screen and a vacuum vessel. It

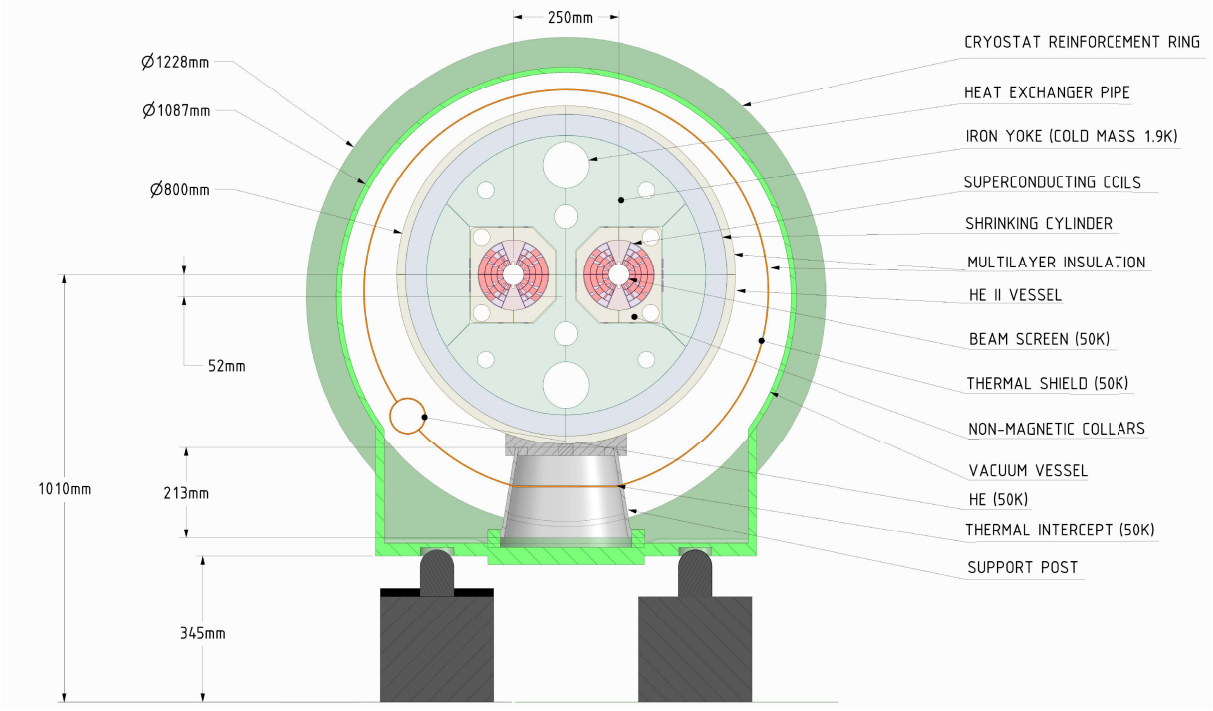

Figure 3.1: Main dipole cross-section.

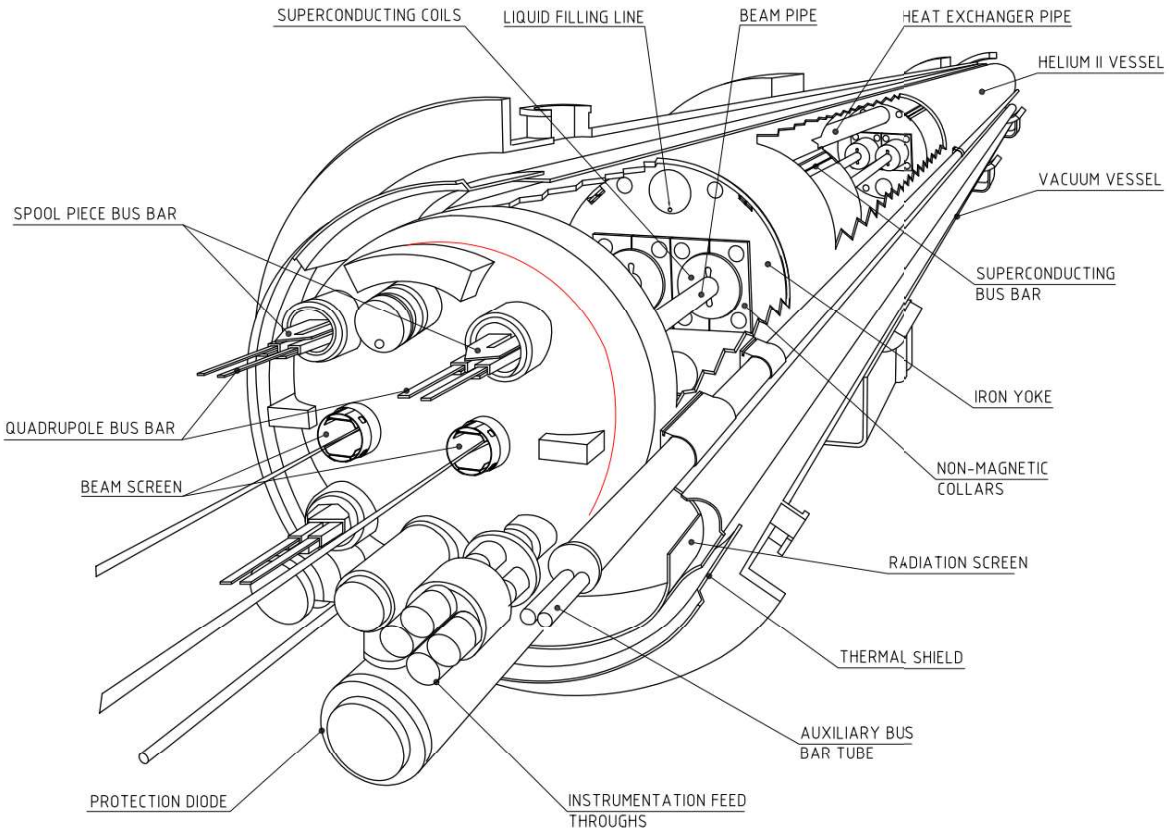

Figure 3.2: 3D-view of main dipole cold mass assembly.

is supported on three feet made from a composite material and a flange is bolted to the vacuum vessel.

All parts between the beam pipe and the shrinking cylinder, which defines the outer envelope of the cold mass, are immersed in superfluid helium at atmospheric pressure and cooled by a heat-exchanger tube, in which two-phase low-pressure helium circulates. The next temperature stage is that of the beam screen, cooled at a reference temperature of 50 K, which is also the temperature level for cooling the thermal screen and the support posts. The fact that the additional intermediate temperature level used in the LHC, in the range between 4 to 20 K, is missing, results in larger static losses from the cold mass and the support posts than in the LHC. The total heat loads of a cryodipole operating in steady state mode are estimated to be about 0.5 W/m at 1.9 K and about 10 W/m at 50 K. The target losses during a full cycle from nominal field, down to injection and up to nominal field again, which mainly come from the magnetisation of the superconductor, are set to 5 kJ/m at 1.9 K for the two apertures. The operating field of 16 T is generated by a current of 11441 A in a coil with a physical aperture of 50 mm. The distance between the axis of the two apertures is 250 mm. The magnet design is described in [152]. The main parameters of the MD, including the expected field quality, are listed in Table 3.1.

Table 3.1: Main dipole parameters.

Item	**Unit**	**Value**
Number of units		4668
Operating field	T	16.0
Coil physical aperture	mm	50.0
Operating current	A	11441
Operating temperature	K	1.9
Magnetic length @ 1.9K	mm	14069
Stored energy at 16 T (entire magnet)	MJ	37
Self-inductance at 16 T (entire magnet)	mH	570
Field margin on the load line at 16 T	%	14
Magnetisation losses (two apertures) over a full excitation cycle	kJ/m	5
Distance between aperture axes at 1.9K	mm	250
Number of coil turns per aperture		200
Surface of conductor (2 apertures)	cm^2	131
Cold mass length beam pipe flange-to-flange at 1.9K	m	15.8
Mass of the cold mass	t	55
Mass of the cryostat	t	6
Geometric field harmonics b_2,b_3,b_4, b_5	units	3.7, -2.4, 0.95, 0.30
Contribution of persistent currents b_2,b_3,b_4, b_5	units	2.0,-23,-0.16,4.9
Contribution of saturation b_2,b_3,b_4, b_5	units	-3.7,2.5,-0.64,-0.11
Total field harmonics b_2,b_3,b_4, b_5 at injection (1.06 T)	units	5.6,-25,0.79,5.2
Total field harmonics b_2,b_3,b_4, b_5 at nominal field (16 T)	units	0.025,0.11,0.31,0.18
Random harmonics b_2,b_3,b_4, b_5	units	0.93,0.67,0.47,0.28
Random harmonics (skew) a_2,a_3,a_4, a_5	units	1.1,0.75,0.48,0.33

The so called "margin on the load line" has been set to 14%, which is the same as the one adopted for the LHC at the nominal field of 8.3 T. Each MD aperture has 200 cable turns distributed in one upper and one lower pole, and each pole comprises two double layer (inner and outer) coils. Since the magnetic flux density varies considerably in the coil (it is much higher in the inner than in the outer pole), the design exploits the principle of grading (see below). The inner pole comprises 32 turns of a 0.5° keystoned Rutherford cable, made from 22 strands of 1.1 mm diameter, the outer pole has 68 turns of a 0.5° keystoned Rutherford cable, made from 38 strands of 0.7 mm diameter (see Table 3.3). The conductor distribution and the field amplitude in the coil is shown in Fig. 3.3, where one quarter of an aperture is shown. The coil cross-section is asymmetric, to compensate the quadrupole component of the

magnetic field coming from the interaction between the two magnet apertures.

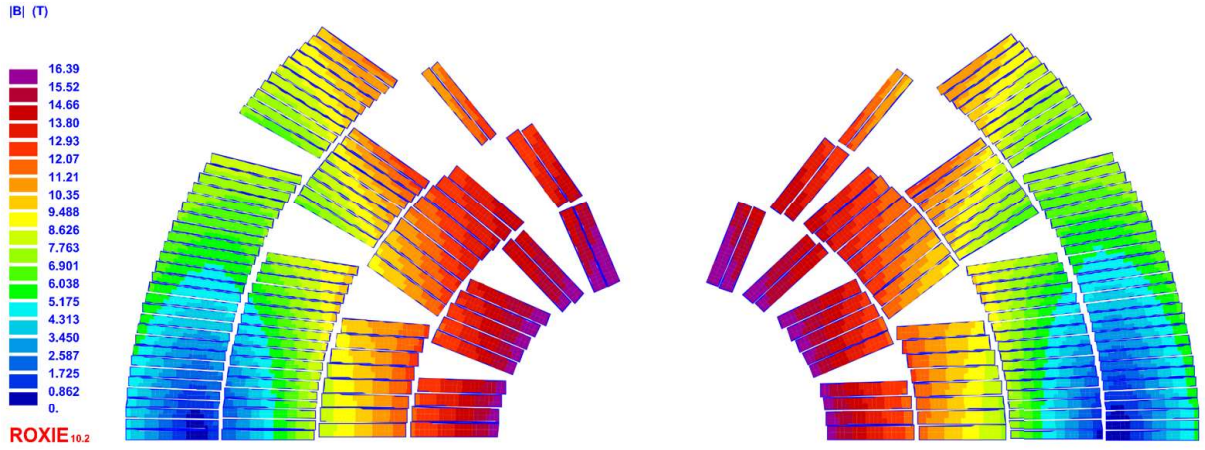

Figure 3.3: Conductor distribution and field amplitude in the coil (half aperture).

The current density in the outer coil is larger than that in the inner coil because the two coils are connected in series and the cable in the inner layers has a larger conductor area than that in the outer layers. Thanks to grading, the current density, where the magnet field is lower, is increased, resulting in a considerable saving of conductor for a given margin on the load line. The structure is based on the so-called "key and bladders" concept together with the use of an aluminium cylinder surrounded by a stainless steel welded shell. The aluminium shell provides the increase of coil loading required from assembly to the operational temperature and during magnet powering. The stainless shell, as well as adding stiffness to the structure, provides helium tightness, alignment fiducials and support for the magnet end covers. The CM assembly and its main components are shown in Fig. 3.4.

The field distribution in the magnet cross section for a central field in the magnet aperture of 16 T, is shown on the left side of Fig. 3.5. The von Mises stress distribution in the structure at the same field of 16 T is shown on the right side of the same picture. The detail of the stress distribution in the coil cross section is shown in Fig. 3.6. Concerning the electromagnetic section, the ferromagnetic yoke is saturated, thus producing a stray field which is about 0.1 T at the boundary of a non-magnetic cryostat. Concerning the structural section, the coil remains entirely under azimuthal compression (with a minimum pressure of 6 MPa) up to the 16 T field amplitude. In these conditions the peak stress on the coil does not exceed 180 MPa. The stress in the other part of the structure remains well below the limits of the magnet components.

Each magnet will be cold tested prior to installation in the tunnel. Depending on its training performance, the magnet may also be submitted to a thermal cycle to confirm that, once installed, the magnet can be powered up to nominal field without experiencing training quenches. As was successfully done for the LHC, a warm-cold magnet measurement correlation will be established, based on the statistics from pre-series magnets. All series magnets will be then magnetically measured warm. Only a small percentage of them will also measured at operating (cryogenic) temperatures.

3.2.3 Field Quality

The field error naming convention follows the one adopted for the LHC [153]. The systematic field error values are deterministic and computed with ROXIE: they comprise a geometric contribution, a contribution coming from persistent currents and the effect of saturation of the ferromagnetic yoke. The contribution from the persistent currents [154] has been computed using the conductor parameters of Table 3.2 and assuming that artificial pinning has been implemented which allows to reduce the critical current (thus the magnetisation) at low fields. Considering that it is very unlikely that a perfect point

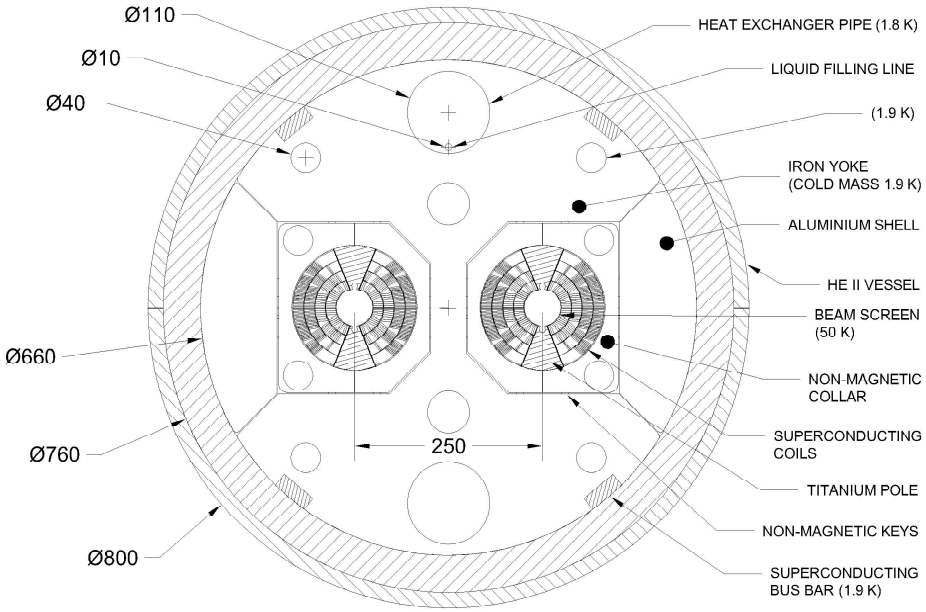

Figure 3.4: Main dipole cold mass.

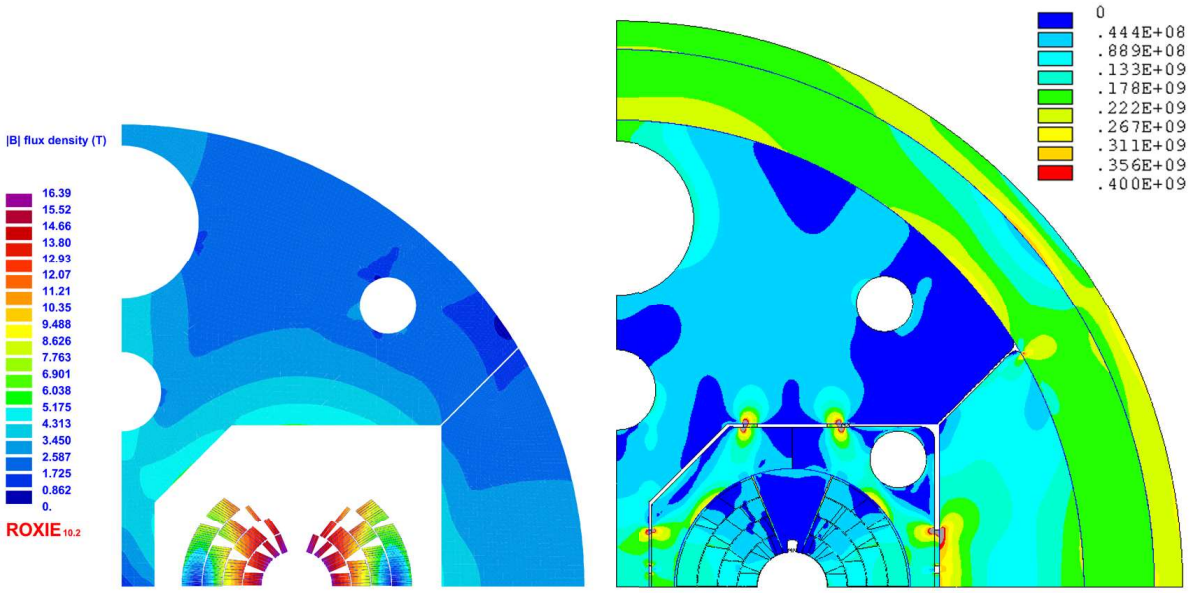

Figure 3.5: Electromagnetic (left) and structural (right) cross-section for a central field of 16 T.

pinning can be achieved, the contribution reported in Table 3.1 has been obtained considering 50% of perfect point pinning. The random values are due to the spread of the geometric and persistent current contributions. The geometric random errors have been determined by means of Monte-Carlo simulations which include a random displacement of the coil blocks with a root-mean-square (RMS) amplitude d = 50 µm. The random errors due to persistent currents have been computed by means of a Monte-Carlo

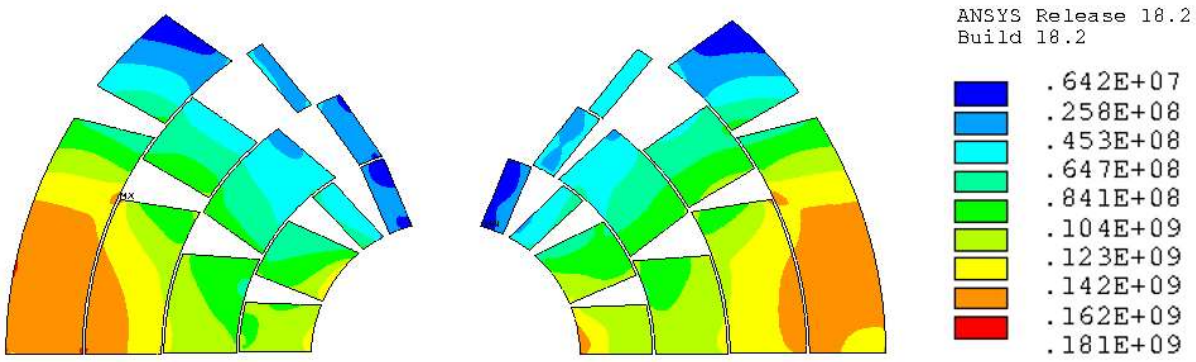

Figure 3.6: Stress distribution (von Mises) in the coil for a central field amplitude of 16 T.

simulation including a standard deviation of magnetization between magnets of ± 5 %. The uncertainty errors are linked to the production line. At this stage, it is assumed, as for HL-LHC, that the production is uniform; therefore the uncertainties are equal to the random values. Further optimisation is on-going to passively correct the b_3 error from persistent currents by using iron shims. The yoke shape will also be further optimised to minimise the saturation effects.

3.2.4 Magnet Protection

The magnet and its protection system are conceived to limit the hot spot temperature to below 350 K in the case of a quench and the peak voltage to ground in the coil below 2.5 kV. This voltage limit includes up to 1.2 kV due to the quench evolution in the magnet itself and up to 1.3 kV from the circuit. The protection system can be based on the coupling-loss-induced quench method (CLIQ), on quench-heaters alone or on a combination of both. On paper, all options effectively protect the magnets within the above limits [155]. Experiments on FCC models and prototypes will allow to understand in real conditions if CLIQ can be implemented with the required reliability and redundancy for every quench situation. For the reasons above, though it is believed that CLIQ has the potential to quench the entire magnet in 30 ms after the initiation of a quench (time delay), the 16 T magnets have been designed assuming a time delay of 40 ms, which is compatible with the use of quench-heaters.

3.2.5 Other Design Options

In addition to the baseline design of the cosine-theta coil type, other design options have been studied in detail; they will be tested experimentally in the coming years. These other designs are the block-type [156], the common-coil [157] and the canted-cosine-theta (CCT) [158] configurations. All options have been explored considering the same assumptions, in particular concerning the magnet aperture (50 mm), the field amplitude (16 T), the conductor performance (assuming the availability of a conductor with a target critical current density of 1500 A/mm2 @ 4.2 K @ 16 T, corresponding to 2300 A/mm2 @ 1.9 K @ 16 T), the margin on the load line (>14%) and the allowed mechanical constraints on the superconducting coil (<150 MPa at warm and <200 MPa at cold). The electromagnetic cross-section of each of these options is shown in 3.7. Their salient features, with respect to the baseline cosine-theta, are shown in Table 3.2.

Each of these alternatives features some interesting characteristics which may have a potential to become competitive to the baseline cosine-theta design in terms of performance, in particular if they would allow to operate at a lower margin on the load-line, thus reducing the required amount of conductor.

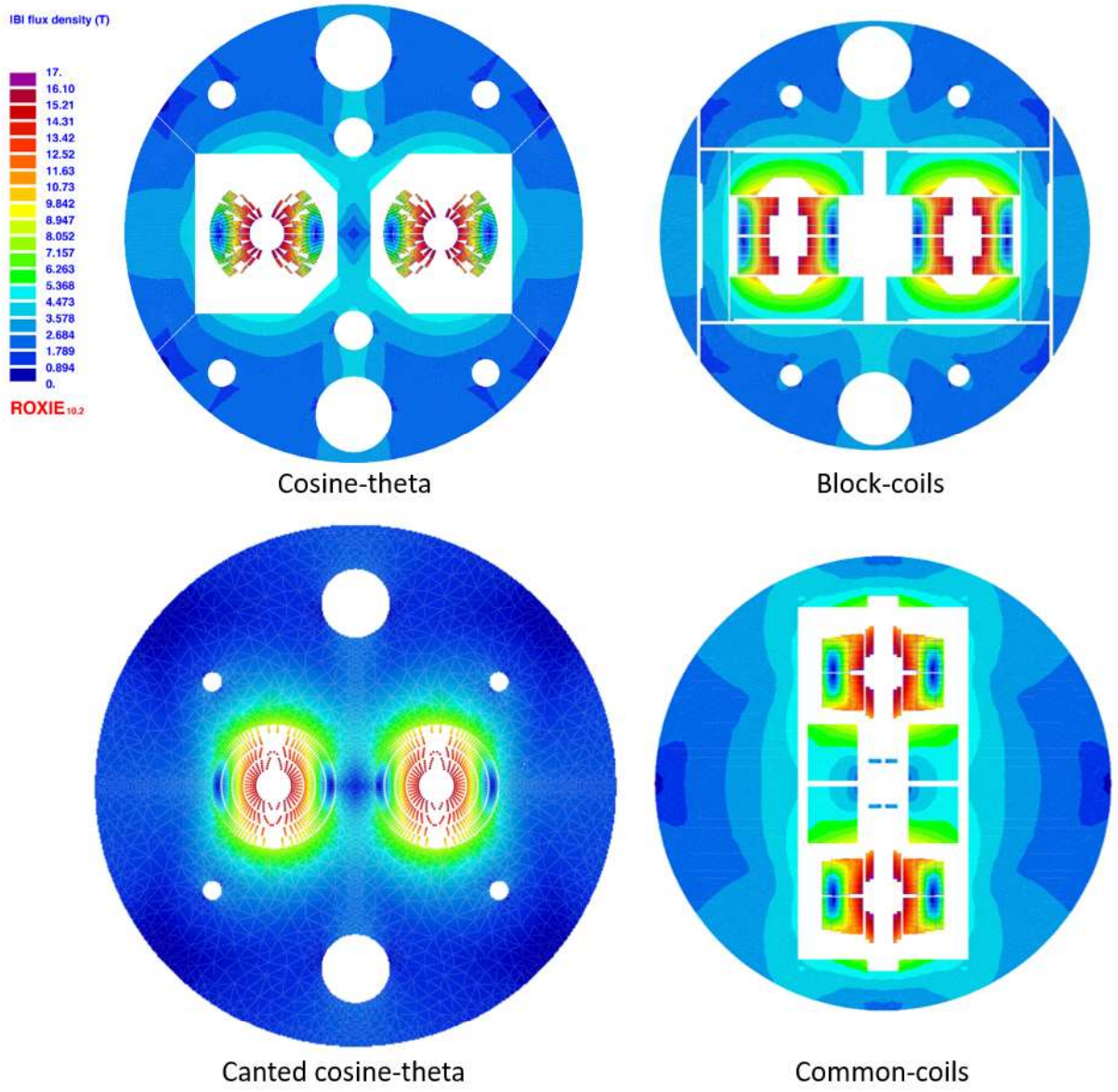

Figure 3.7: Electromagnetic cross sections of the 16 T dipole design variants.

3.2.6 Low Temperature Superconductors

The 16 T dipole magnets for the FCC rely on Nb_3Sn. Experience has been gained in the use of this technology in both the U.S and Europe, not only on R&D magnets but, more recently also on accelerator magnets, thanks to the HL-LHC project. Both the electrical performance and filament size are currently beyond state-of-the-art for Nb_3Sn wire. A dedicated R&D programme has been launched worldwide, with some promising results already [159]. This programme has three phases. In the first phase, the focus is on increasing the critical current by 50% with respect to HL-LHC (1500 A/mm^2 at 4.2 K and 16 T), maintaining high RRR (150). This requires a major breakthrough and work on novel methods, such as artificial pinning centres (APC), grain refinement and architectures. In the second phase, the conductor will be optimised to reduce the magnetisation, in particular at low fields, by modifying the effective filament diameter and possibly using APC. The third phase can be considered the preparation to industrialisation, focusing on achieving long unit length (5 km) and competitive cost (5 kEuro/kAm at 4.2 K and 16 T). As reported in [159], despite the short time since the start of the program, high-performing Nb_3Sn conductors have been already produced by new collaborating partner institutes and

Table 3.2: Salient features of design options for 16 T magnets.

Parameter	**Cos-theta**	**Block-coil**	**CCT**	**Common-coil**
Peak field on conductor [T]	16.40	16.73	16.35	16.57
Operating current [A]	11441	10176	18135	15880
Inductance @ 16 T [mH/m]	38	48	18	26
Outer yoke diameter [mm]	660	616	750	650
Mass of conductor [kg/m]	115	120	148	145

companies, achieving a J_c performance in the order of the specification for HL-LHC. Work performed on grain refinement and APC has shown promising results, with nearly doubling the J_c at 12 T, 4.2 K on small samples. Finally, to improve the training of magnets, one considers introducing materials with high heat capacity (Gd_2O_3) directly within the Nb_3Sn wire.

Two distinct conductors are used for the 16 T dipoles: a high-field (HF) conductor used for the inner pole and a low-field (LF) conductor used for the outer pole. The parameters of the HF and LF conductors are summarised in Table 3.3. It is assumed that the insulated conductor can be subjected to pressures of up to 150 MPa at ambient temperature and 200 MPa when cold, without experiencing an irreversible degradation. Based on the information coming from tailored experiments and from magnet tests, these values are considered to be challenging but realistic. Finally, due to the high J_c, the large filament diameter and the large amplitude of a magnet cycle, the magnetisation losses of these magnets have a considerable impact on the design of the cryogenic system, which assumes 5 kJ/m at 1.9 K for the two apertures. This limit can be respected with filament diameters of around 20 µm and if new manufacturing techniques have been developed, e.g. the aforementioned APC, and if the reset current during the machine powering cycle will be optimised.

Table 3.3: Target parameters for the main dipole conductor.

Property	**Unit**	**Value**
Wire		
Critical current density at 16 T and 1.9 K	A/mm^2	1500
Strand diameter HF conductor	mm	1.1
Strand diameter LF conductor	mm	0.7
Filament size HF conductor	µm	20
Filament size LF conductor	µm	20
Cu/nonCu HF conductor		0.8:1
Cu/nonCu LF conductor		2.1:1
Cable		
Number of strands HF cable		22
Number of strands LF cable		38
Width of HF cable	mm	13.2
Width of LF cable	mm	14.0
Keystone angle of HF/LF cable	degrees	0.5
Average thickness of HF cable	mm	1.950
Average thickness of LF cable	mm	1.265

3.2.7 Superconducting Main Quadrupole

The main quadrupoles (MQ) of FCC are twin-aperture magnets based on a cosine-2theta coil configuration assembled in a 20 mm thick helium II vessel. Their design is detailed in [160]. The cooling system

and the cryogenic features in the iron yoke are linked to the MD magnet characteristics. Like the MD magnet, the inter-beam distance is 250 mm and the physical aperture is 50 mm in diameter. Each aperture is mechanically independent from the other due to the use of a collar-and-key mechanical assembly. The main parameters of the MQ are listed in Table 3.4. Each double pancake is made of 18 turns of Nb_3Sn Rutherford cable with a 0.4° keystone angle. The cable consists of 35 strands, 0.85 mm in diameter; the filament size is 20 µm. The CLIQ system protects the magnet with a hot spot limited to 350 K and a peak voltage to ground below 900 V.

Table 3.4: Main quadrupole parameters.

Item	**Unit**	**Value**
Number of units		744
Operating gradient	T/m	367
Coil physical aperture	mm	50.0
Peak field	T	10.51
Operating current	A	22500
Operating temperature	K	1.9
Magnetic length @ 1.9K	mm	7063
Stored energy at 16 T (entire magnet)	MJ	3.7
Self-inductance at 16 T (entire magnet)	mH	14.4
Field margin on the load line at nominal	%	20
Temperature margin at nominal	K	4.6
Distance between aperture axes at 1.9K	mm	250
Number of coil turns per aperture		72
Mass of the cold mass	t	17
Total field harmonics at nominal b_6,b_{10}	units	-0.47, 0.41
Total field harmonics ai injection b_6,b_{10}	units	-22.3, 2.40

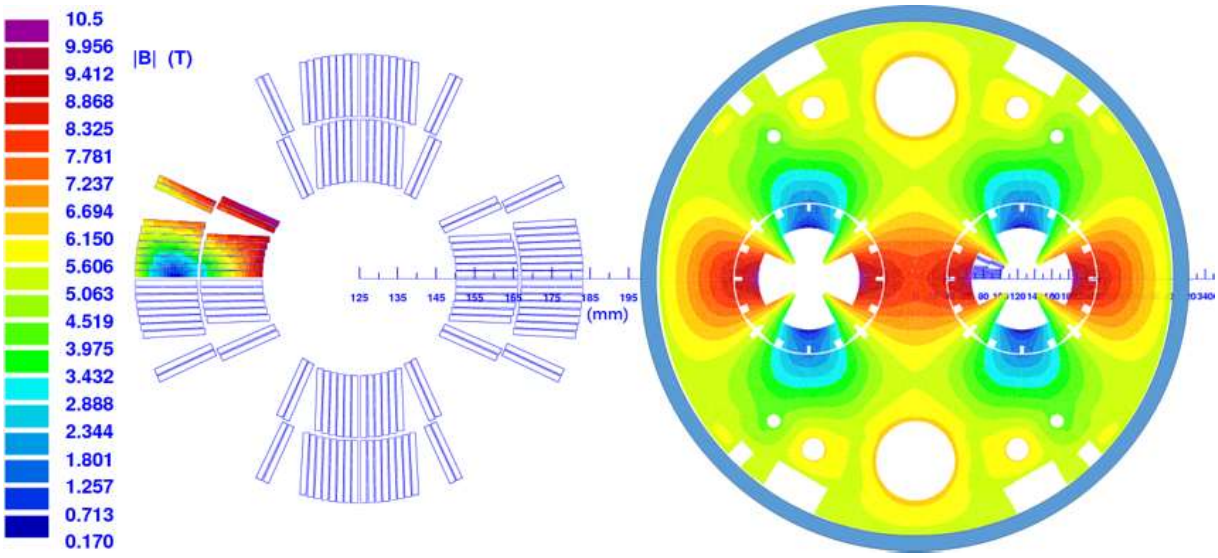

Figure 3.8: (left) Conductor distribution and magnetic field [T] in the coil (right) iron yoke, steel collar layout and HeII vessel.

3.2.8 Other Magnets in the Arcs

For the FCC-hh, the FODO cell length in the arc was chosen to be 213 m, roughly double the length of the LHC FODO cell. The FCC-hh has 8 long arcs, each with 36.5 FODO cells, and 4 short arcs, each with 15 FODO cells. Each FODO cell has 12 dipoles and 2 Short Straight Sections (SSS). As in the LHC, each SSS contains one MQ, and sextupole (MS) and dipole corrector magnets (MC). Depending on the SSS location in the arc, there may be in addition octupole corrector magnets (MO), tuning quadrupoles (MQT) or skew quadrupoles (MQS). It is planned to have 3510 MB-MB, 704 MB-SSS and 704 SSS-MB interconnections in the arcs. The magnet types and their main parameters are listed in Table 3.5. All these magnets, except the DIS quadrupole (MQDA), use Nb-Ti technology. The MQDA relies on Nb_3Sn. The space required for the interconnections and the magnet extremities is summarised in Table 3.6, which shows the target distance between the magnetic ends of the different magnets.

Table 3.5: Other magnets in the Arcs.

Magnet type	**Technology**	**Number**	**Strength**	**Length**
Lattice sextupoles (MS)	NbTi	696	7000 T/m^2	1.2 m
Lattice octupoles (MO)	NbTi	480	200000 T/m^3	0.5 m
Dipole correctors (MCB)	NbTi	792	4 T	1.2 m
Trim quadrupoles (MQT)	NbTi	120	220 T/m	0.5 m
Skew quadrupoles (MQS)	NbTi	96	220 T/m	0.5 m
MCS	NbTi	2x4668	3000 T/m^2	0.11 m
DIS quadrupole (MQDA)	Nb_3Sn	48	360 T/m	9.7 m
DIS trim quadrupole (MQTL)	NbTi	48	220 T/m	2.0 m

Table 3.6: Distances between magnets (magnetic lengths).

Magnet types	**Distance (m)**	**Remarks**
MB-MB	1.5	This considers 0.11 m long MCS
MB-BPM	1.3	BPM stands for beam position monitor
MQ-other	0.35	Other magnetic elements in SSS
Other-other	0.35	

3.2.9 Low-beta Triplets

The low-beta triplets are composed of quadrupole magnets and corrector magnets. There are two types of low-beta triplets for installation in the high- and low-luminosity interaction regions, respectively. The magnet types and their main parameters are listed in Table 3.7. The target distance between the magnetic length of each of these magnets is two metres, ignoring the corrector magnets.

Table 3.7: Low-beta Triplets

Magnet type	**Technology**	**Number/IP**	**Strength**	**Length**	**Aperture**
Q1 high lumi	Nb_3Sn	4	130 T/m	14.3 m	164 mm
Q2 high lumi	Nb_3Sn	8	105 T/m	12.5 m	210 mm
Q3 high lumi	Nb_3Sn	4	105 T/m	14.3 m	210 mm
Q1 low lumi	Nb-Ti	4	270 T/m	10.0 m	64 mm
Q2 low lumi	Nb-Ti	4	270 T/m	15.0 m	64 mm
Q3 low lumi	Nb-Ti	4	270 T/m	10.0 m	64 mm

The magnets around the collision points will be exposed to high radiation levels which may adversely affect their performance. It is assumed that the conductor performance can be maintained until a displacement-per-atom (DPA) value of 2×10^{-3} and that the magnet insulation can withstand an accumulated radiation dose of 30 MGy. These values may be exceeded over the machine lifetime, going up to 40 to 50 MGy assuming the use of the baseline 35 mm thick tungsten shield. Some optimisation to reduce this value in the collision optics is ongoing. This radiation load may be still affordable if either a more radiation resistant impregnation system is developed in the magnets or if the triplet magnets are replaced once in the machine lifetime. Furthermore, the estimated static heat load using the baseline shield and at the nominal operation conditions, is 4.5 mW/cm^3, which corresponds to a temperature increase of the coil of about 0.5 K.

3.2.10 Other Magnets

Depending on their location, the matching and dispersion suppressor quadrupoles have a cross-section similar to the MQ but with apertures increased to up to 70 mm. Around 156 matching quadrupoles are distributed as follows: 96 in the dispersion suppressors, 16 in the high-luminosity experiment insertions, 20 in the low-luminosity experiment insertions and injections, 6 in the injection and extraction sections, 8 in the RF section and 10 in the collimation section. Furthermore, 48 trim quadrupoles are installed in the 16 dispersion suppressors. The same type of magnets as those in the LHC are required in the collimation insertion. However, the radiation load in the betatron collimation region is large. Normal-conducting dipole magnets with bedstead coils are proposed in order to reduce the radiation dose by one order of magnitude compared to magnets with racetrack coils. Finally, there are 12 normal-conducting and 8 superconducting separation and recombination dipoles. These magnets are listed in in Table 3.8.

Table 3.8: Other magnets

Magnet type and location	**Tech**	**Number**	**Strength**	**Length**	**Aperture**
Separation dipoles D1 high lumi	Copper	6/IP	1.91 T	3×12.5 m	168 mm
Recombination dipoles D2 high lumi	Copper	6/IP	1.91 T	3×12.5 m	58 mm
Separation dipoles D1 low lumi	Nb_3Sn	4/IP	12 T	12.5 m	100 mm
Recombination dipoles D2 low lumi	Nb_3Sn	4/IP	10 T	15.0 m	60 mm
Q4 high lumi	Nb-Ti	2/IP	175 T/m	9.1 m	70 mm
Q5 high lumi	Nb-Ti	2/IP	260 T/m	12.8 m	60 mm
Q6 high lumi	Nb-Ti	2/IP	225 T/m	12.8 m	60 mm
Q7 high lumi	Nb_3Sn	4/IP	400 T/m	14.3 m	50 mm
Q4 low lumi	Nb-Ti	2/IP	200 T/m	9.1 m	70 mm
Q5 low lumi	Nb-Ti	2/IP	275 T/m	12.8 m	50 mm
Q6 low lumi, extraction side	Nb-Ti	1/IP	170 T/m	12.8 m	50 mm
Q6 low lumi, injection side	Nb-Ti	2/IP	170 T/m	9.1 m	70 mm
Q7 low lumi	Nb-Ti	2/IP	84 T/m	12.8 m	50 mm
Q8 low lumi	Nb-Ti	2/IP	120 T/m	9.1 m	70 mm
MCB2 (single ap) high lumi	Nb-Ti	8	3 T H/V	1.3 m	240 mm
MCB3 (single ap) high lumi	Nb-Ti	4	3 T H/V	1.3 m	240 mm
MCB4h high lumi	Nb-Ti	4	3 T	3 m	70 mm
MCB4v high lumi	Nb-Ti	4	3 T	3 m	70 mm
Orbit Correctors low lumi	Nb-Ti	12	3 T	1 m	64 mm